Electrochemical lithiation of the CeNiC$_2$ compound

Vasyl KORDAN[1], Mykola HEMBARA[1], Volodymyr PAVLYUK[1], Bogdan KOTUR[1]*

[1] *Department of Inorganic Chemistry, Ivan Franko National University of Lviv,*
Kyryla i Mefodiya St. 6, 79005 Lviv, Ukraine
* *Corresponding author. Tel.: +380-32-2600388; e-mail: bohdan.kotur@lnu.edu.ua*

Electrochemical lithiation of CeNiC$_2$ was carried out in a Swagelok-type cell with a positive electrode containing LiCoO$_2$ over 51/50 cycles of lithiation/delithiation. The crystal structure of CeNiC$_2$ (structure type CeNiC$_2$, Pearson symbol *oS*8, space group *Amm*2) before and after lithiation was investigated by X-ray diffraction. The electrodes containing the ternary carbide were examined by scanning electron microscopy and energy-dispersive X-ray spectroscopy. The crystal structure of CeNiC$_2$ remained very stable toward electrochemical lithiation. The volume of the unit cell after 51/50 lithiation/delithiation cycles decreased by only 0.06 %. A small amount of lithium, up to 0.115 Li per formula unit, was reversibly incorporated into CeNiC$_2$. The electrochemical lithiation process included two reactions: 1) insertion of Li into suitable voids and channels of near-surface layers of CeNiC$_2$, and 2) partial decarbonization of the electrode. The composition and morphology of the grains of the electrode material changed only slightly. Small amounts of Li$_z$C$_y$, Ce$_{22.7}$Ni$_{21.6}$O$_{55.7}$ and Li$_2$O were detected as by-products of the lithiation. The lithiation mechanism of ternary carbides containing a rare earth and a 3*d*-element depends on the stoichiometry and peculiarities of the crystal structure.

Ternary carbides / X-ray diffraction / Crystal structure / Electrochemical lithiation

Introduction

Electrode materials on the basis of intermetallic compounds have practical application in the production of modern energy storage materials. Some intermetallic compounds containing *d*- and *p*-elements have the ability to intercalate lithium atoms in their structures, when these have sufficiently large octahedral voids and/or layered character [1,2]. For this reason they can be potential materials for negative electrodes in various electrochemical devices.

Inclusion of Li-atoms upon electrochemical lithiation into voids or other positions in the crystal structures of basic intermetallic compounds leads to the formation of solid solutions. Electrochemical lithiation of ternary carbides comprising both rare-earth (*f-*) and *d*-transition elements have hardly been studied. In our previous investigation [3] we made an attempt to intercalate Li into the structure of Ce$_2$Mn$_{17}$C$_{1.77}$. This ternary carbide crystallizes in the rhombohedral (trigonal) Pr$_2$Mn$_{17}$C$_{1.77}$-type structure (Pearson symbol *hR*66, space group *R*-3*m*), which is a derivative of the Th$_2$Zn$_{17}$-type structure. Electrochemical lithiation was carried out in a Swagelok-type cell with a positive electrode containing LiCoO$_2$. However, after 30 cycles of lithiation, decarbonization of the ternary carbide was observed, accompanied by a decrease of the cell volume from 847.9(2) Å^3 to 842.7(5) Å^3, $\Delta V/V$ = -0.6 %, formation of α-Li$_2$C$_2$ and Li$_x$C$_y$ carbides, and amorphization of the Ce$_2$Mn$_{17}$ alloy.

In the present work we report the results of electrochemical lithiation of another ternary carbide – CeNiC$_2$. This phase crystallizes in its own type of structure: Pearson symbol *oS*8, space group *Amm*2, a = 3.875, b = 4.552, c = 6.162 Å [4]. It belongs to the group of carbometalates, a large group of ternary carbides with strong *T*-C (*T* = *d*-transition element) bonds and occurrence of [T_yC$_z$]$^{n-}$ anionic fragments in their crystal structures [5]. The compound CeNiC$_2$ is already present in as-cast alloys, is very stable in air and has [Ni(C$_2$)]$_\infty^{n-}$ anionic layers in its structure [5]. This phase could be interesting for energy storage applications, *i.e.* for electrochemical lithiation by reversible lithium intercalation.

Experimental

An 1.5 g alloy of composition Ce$_{25}$Ni$_{25}$C$_{50}$ was prepared by arc-melting pieces of the initial elements

cerium, nickel and carbon with a purity not less than 99.9 wt.% (Alfa Aesar, A. Johnson Matthey Company) under an argon atmosphere purified with a molten Ti getter on a water-cooled copper hearth, using a non-consumable tungsten electrode. A small mass excess of carbon of up to 2 wt.% of the nominal weight was added to avoid possible losses during the preparation of the alloy. During the melting procedure the weight losses were <2.0 wt.% of the total mass of the ingot. Subsequently, the alloy was annealed in an evacuated quartz ampoule at 600°C for 30 days.

Phase analysis of the alloys and crystal structure refinements were performed with the help of the WinXPOW [6] and WinCSD software packages [7], on powder X-ray diffraction (XRD) data obtained using a STOE STADI P (Cu $K\alpha_1$-radiation) powder diffractometer. Scanning electron microscopy (SEM), qualitative and quantitative composition analyses of powders, were performed by energy-dispersive X-ray spectroscopy (EDX) with an elemental analyzer REMMA-102-02 coupled to the SEM.

Electrochemical insertion of lithium into the ternary phase CeNiC$_2$ was carried out in 2-electrode prototype Swagelok-type cells that consisted of a negative electrode containing 0.3 g of the studied alloy and a positive electrode containing 0.4-0.5 g LiCoO$_2$ (structure type NaFeO$_2$, space group R-3m). The separator consisted of pressed cellulose with large specific surface area, to ensure electrolyte absorption (1 M solution of Li[PF$_6$] in a solvent mixture of ethylenecarbonate-dimethylcarbonate 1:1). Testing of the batteries was carried out in the galvanostatic regime (1.0 mA/cm^2) over 50 cycles. A galvanostat MTech G410-2 [8] was used to measure the electrochemical characteristics of the battery prototypes.

Results and discussion

Full-profile analysis of the crystal structure of CeNiC$_2$ before and after lithiation was carried out using the powder XRD Rietveld refinement method. XRD profiles of the initial sample and after 51 lithiation / 50 delithiation cycles are presented in Fig. 1. They are similar, but with some changes in the low-angle region (up to $2\theta \sim 20^\circ$). The refined atomic and isotropic displacement parameters of CeNiC$_2$ in the initial homogenized sample and after 51/50 cycles of electrochemical lithiation/delithiation are shown in Table 1, while details of the structure refinements are listed in Table 2. A slight decrease of the unit-cell parameters and cell volume of CeNiC$_2$ occurred after lithiation. The atomic coordinates and displacement parameters of the two samples are very similar. This indicates stability of the crystal structure of CeNiC$_2$ upon lithiation and a very limited lithium penetration into the carbide. Interatomic distances in the CeNiC$_2$ structure before and after lithiation are presented in Table 3. The differences between the values of the same interatomic distances are within the error bars. This is also valid for the C–C bond lengths in the structure: dC–C = 1.41(2) Å and 1.39(2) Å, before and after lithiation, respectively. For comparison, the atomic radii for metallic cerium and nickel are δCe = 1.83 Å and δNi = 1.24 Å, while those for single carbon atoms, covalent single- and double-bonded C$_2$ are δC = 0.92 Å, 0.77 Å and 0.67 Å, respectively [9]. In the structure of the CeNiC$_2$ carbide the carbon atoms form double-bonded C=C pairs, which are very stable toward lithiation, differently from the structure of Ce$_2$Mn$_{17}$C$_{1.77}$ where single carbon atoms occupy octahedral voids in the structure [3].
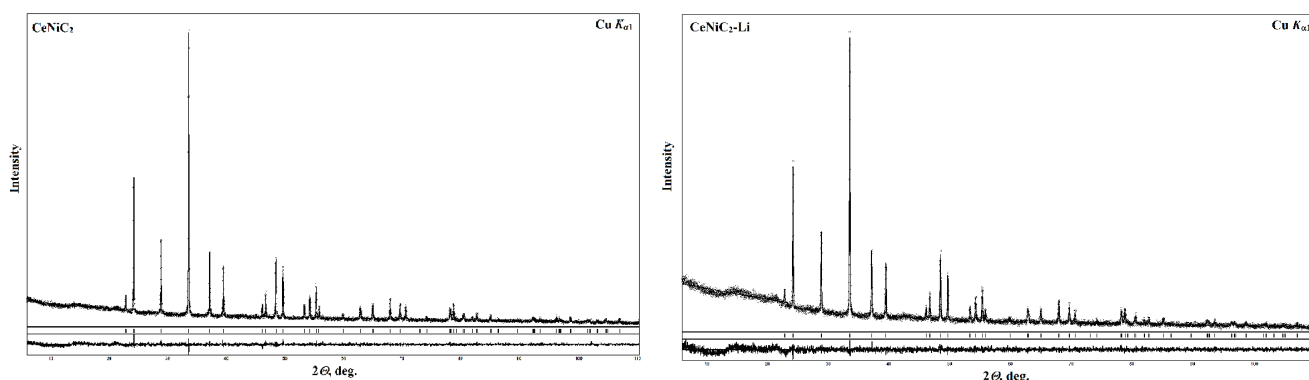

Fig. 1 Measured (dots) and calculated (line) profiles and their difference plots (bottom) of the XRD pattern of the Ce$_{25}$Ni$_{25}$C$_{50}$ sample before (left) and after 51/50 cycles of electrochemical lithiation/delithiation (right). The positions of the Bragg peaks are indicated by vertical lines between the measured and difference profiles.

Table 1 Atomic and isotropic displacement parameters for the CeNiC$_2$ compound before (first row) and after 51/50 cycles of electrochemical lithiation/delithiation (second row).

Atom	Wyckoff position	x	y	z	B_{iso}, Å^2
Ce	2*b*	½	0	0.3849(5)	0.89(3)
				0.3844(6)	1.09(5) [a]
Ni	2*a*	0	0	0.000 [b]	1.29(9)
				0.000 [b]	0.78(1) [a]
C	4*d*	0	0.345(4)	0.177(3)	1.000 [b]
			0.348(4) [a]	0.179(3) [a]	1.000 [b]

[a] after 50 cycles of sample lithiation; [b] fixed during the refinement

Table 2 Details of the refinement of the crystal structure of CeNiC$_2$ before and after 51/50 cycles of electrochemical lithiation/delithiation.

Phase	CeNiC$_2$	CeNiC$_2$–Li$_x$
Space group	*Amm*2	
Z	2	
a, Å	3.87614(9)	3.8756(2)
b, Å	4.54888(9)	4.5481(2)
c, Å	6.1611(1)	6.1596(2)
V, Å^3	108.633(7)	108.57(1)
Calculated density, g·cm^{-3}	6.8123(5)	6.8162(7)
Radiation and wavelength, Å	Cu $K\alpha_1$; 1.54056	
2θ, ° and $\sin\theta/\lambda$, Å^{-1}	110.64; 0.534	
Zero shift	-0.0003	-0.0005
Preferred orientation	1.68(3) [1 0 0]	1.75(4) [1 0 0]
R_B	4.40	5.16
R_P	4.44	4.81
GooF	1.51	1.33
Scale factor	0.09823(1)	0.09301(2)

Table 3 Interatomic distances and coordination numbers of atoms in the crystal structure of the CeNiC$_2$ compound before and after 51/50 cycles of electrochemical lithiation/delithiation.
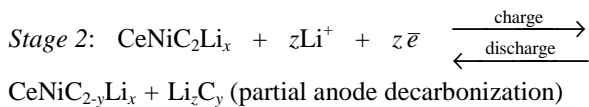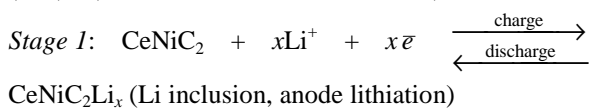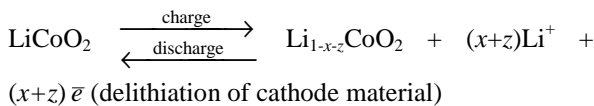
	CeNiC$_2$			CeNiC$_2$–Li$_x$	
Atoms	Interatomic distance d, Å	Coordination number (CN)	Atoms	Interatomic distance d, Å	Coordination number (CN)
Ce – 4C	2.738(2)		Ce – 4C	2.743(3)	
– 4C	2.805(1)		– 4C	2.805(2)	
– 2Ni	3.063(1)	20	– 2Ni	3.061(1)	20
– 4Ni	3.071(2)		– 4Ni	3.071(1)	
– 4Ce	3.829(3)		– 4Ce	3.828(4)	
– 2Ce	3.876(1)		– 2Ce	3.874(2)	
Ni – 2C	1.911(1)		Ni – 2C	1.928(1)	
– 2C	2.111(2)	10	– 2C	2.095(2)	10
– 2Ce	3.063(1)		– 2Ce	3.061(1)	
– 4Ce	3.071(2)		– 4Ce	3.071(1)	
C – C	1.41(2)	9 [a]	C – C	1.39(2)	9 [a]

[a] CN of C$_2$ pairs

Fig. 2 presents selected charge and discharge curves of the voltage *E versus* the number of incorporated Li atoms (per f.u. CeNiC$_2$) for the prototype of the battery LiCoO$_2$∥CeNiC$_2$. The amount of reversible Li was calculated using Faraday's law. The number of incorporated Li atoms per f.u. CeNiC$_2$ depends on the discharge time. As it is seen from Fig. 2, the electrochemical process of
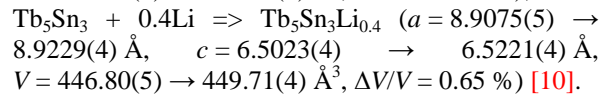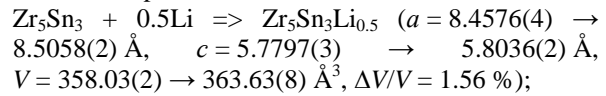
$CeNiC_2$ lithiation consists of two steps (stages): 1) inclusion of small amounts of lithium into the $CeNiC_2$ crystal structure, and 2) subsequent partial decarbonization of the electrode sample. We assumed that all of the current charge is connected with lithiation or delithiation, without interaction of the electrode surface with the electrolyte. Consequently we carried out the calculations considering the charge or discharge time without distinguishing the processes of main reaction (lithiation) and by-reaction (formation of solid electrolyte interphases or other by-products). The series of electrochemical reactions can be presented as:
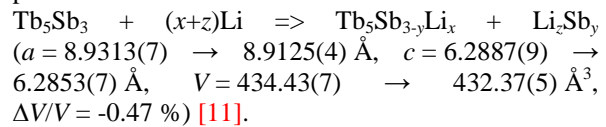
$$LiCoO_2 \xrightleftharpoons[\text{discharge}]{\text{charge}} Li_{1-x-z}CoO_2 + (x+z)Li^+ +$$

$(x+z)\,\bar{e}$ (delithiation of cathode material)

Stage 1: $CeNiC_2 + xLi^+ + x\,\bar{e} \xrightleftharpoons[\text{discharge}]{\text{charge}}$

$CeNiC_2Li_x$ (Li inclusion, anode lithiation)

Stage 2: $CeNiC_2Li_x + zLi^+ + z\,\bar{e} \xrightleftharpoons[\text{discharge}]{\text{charge}}$

$CeNiC_{2-y}Li_x + Li_zC_y$ (partial anode decarbonization)

As a result we observed a slight decrease of the unit-cell parameters: $a = 3.87614(9) \rightarrow 3.8756(2)$ Å; $b = 4.54888(9) \rightarrow 4.5481(2)$ Å; $c = 6.1611(1) \rightarrow 6.1596(2)$ Å; $V = 108.63(7) \rightarrow 108.57(1)$ Å^3. The relative variation of the volume $\Delta V/V$ is only -0.06 %. It characterizes the additive property of this parameter: increasing at the inclusion of Li atoms, and decreasing at the decarbonization by Li.

We recently studied electrochemical lithiation of the binary intermetallic compounds Zr_5Sn_3, Tb_5Sn_3 and Tb_5Sb_3 crystallizing in Mn_5Si_3-type structures [10,11]. In the case of Zr_5Sn_3- and Tb_5Sn_3-containing electrodes we observed inclusion of Li atoms into

voids of the parent structure as the dominant process. As a result filled-up structures of the Hf_5CuSn_3-type were formed. The increase of the unit cell volumes exceeded 0.5 % and we observed pronounced shifts of XRD peaks for the ternary phases, as compared with those of the parent binaries:
$Zr_5Sn_3 + 0.5Li => Zr_5Sn_3Li_{0.5}$ ($a = 8.4576(4) \rightarrow$ 8.5058(2) Å, $c = 5.7797(3) \rightarrow 5.8036(2)$ Å, $V = 358.03(2) \rightarrow 363.63(8)$ Å^3, $\Delta V/V = 1.56$ %);
$Tb_5Sn_3 + 0.4Li => Tb_5Sn_3Li_{0.4}$ ($a = 8.9075(5) \rightarrow$ 8.9229(4) Å, $c = 6.5023(4) \rightarrow 6.5221(4)$ Å, $V = 446.80(5) \rightarrow 449.71(4)$ Å^3, $\Delta V/V = 0.65$ %) [10].

In the case of Tb_5Sb_3-containing electrodes, the main electrochemical reaction was substitution of Li for Sb, and a ternary phase with decreased unit-cell parameters was obtained:
$Tb_5Sb_3 + (x+z)Li => Tb_5Sb_{3-y}Li_x + Li_zSb_y$ ($a = 8.9313(7) \rightarrow 8.9125(4)$ Å, $c = 6.2887(9) \rightarrow$ 6.2853(7) Å, $V = 434.43(7) \rightarrow 432.37(5)$ Å^3, $\Delta V/V = -0.47$ %) [11].

In the present study the relative variation of the unit-cell volume of $CeNiC_2$ after 51/50 cycles of lithiation/delithiation was –0.06 %. The XRD profiles remained practically the same and we assume very limited incorporation of Li into the initial structure of $CeNiC_2$ and decarbonization of the ternary carbide.

We looked for X-ray diffraction peaks from Li_xC_y after 51 cycles of electrode lithiation to confirm partial anode decarbonization, as we did it in our previous study of the ternary carbide $Ce_2Mn_{17}C_{1.77}$ [3]. However, no pronounced peaks from Li_xC_y phases can be detected on the XRD profile (see Fig. 1, right). Nevertheless, the existence of two reactions is evident from the typical discontinuity on the dependence of the prototype battery voltage *versus* the lithium content (Fig. 2). The amount of inserted Li reached 0.010–0.040 Li per formula unit (first short plateaus on charging the battery). It is impossible to establish the exact amount of lithium removed due to
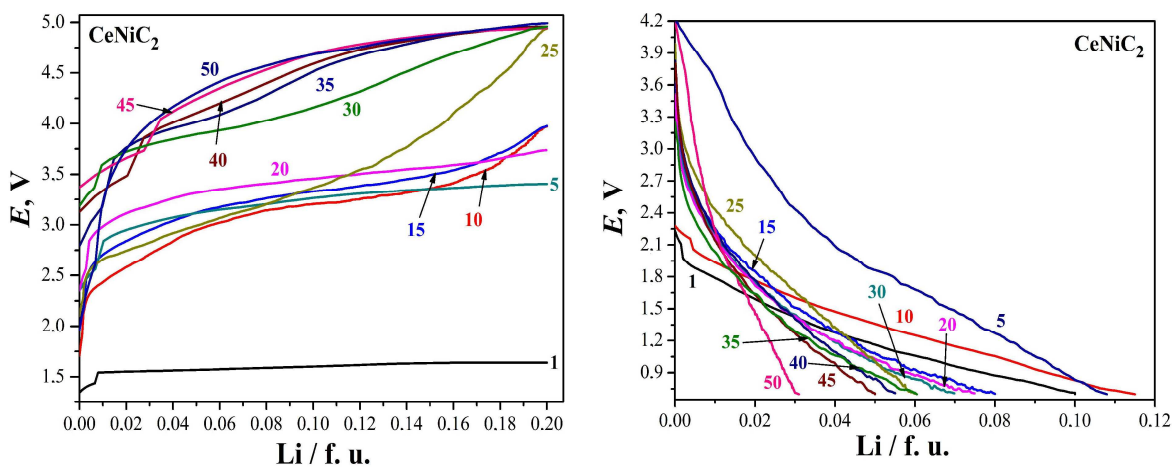

Fig. 2 Selected charge (left) and discharge (right) curves for the prototype of the battery $LiCoO_2$ // $CeNiC_2$. Numbers in color indicate the number of lithiation cycles.

the concomitant decarbonization process. The discharge curves also contain two plateaus (see cycle curves 1, 5, 10). Reverse diffusion of Li from the structure or near-surface layers during the delithiation cycles plays an active role.

Comparing the charge profiles (see Fig. 2, left) we observed that each cycle is different from the others. In general, such electrodes are characterized by an increase of the capacitance due to activation processes (up to 8-10 cycles), then the capacity is stabilized, and after about 30 cycles it decreases. This effect also occurs in non-equilibrium systems without constant diffusion. The processes of Li inclusion and partial decarbonization include a number of microstages (Li absorption on the surface and intercalation into the volume of the electrode, *etc.*), hence we observed a significant change of the potential. During discharge (see Fig. 2, right) the first stage is delithiation of Li$_x$C$_y$ phases, which occurs at the potentials E = 1.9-2.3 V (for 1 and 10 cycles), E = 3.6-4.2 V (for the 5-th cycle) and E = 2.8-3.9 V (for the other cycles). At lower potentials delithiation of the main carbide occurs.

The maximal amount of reversible lithium incorporation reached 0.115 Li/f.u. under the conditions of the experiment. This value possibly explains two origins of active electrochemical lithium (during the discharge process): from the solid solution CeNiC$_{2-y}$Li$_x$ and from Li$_z$C$_y$ phases as by-products of decarbonization. Tian *et al*. [12] reported results of using Li$_2$C$_2$ as cathode material in Li-ion batteries. The theoretical capacity was 1400 mA h/g, while under the experimental conditions they observed a reversible specific capacity of 700 mA h/g. Hence, we explain the two plateaus observed on the discharge curves in Fig. 2 by the electrochemical activity of the Li$_2$C$_2$ carbide. The high lithium mobility depends on the existence of the acetylenide –C≡C– bond. Great interest is devoted to methods of obtaining the binary compound Li$_2$C$_2$ and its polymorphic modifications [13]. The metastable phase β-Li$_2$C$_2$ is characterized by a coarse-grained polycrystalline system and can be stabilized thanks to the nano-grain size effect [14].

Scanning electron microscopy (SEM) was used to observe the topology of the surface of the electrode containing CeNiC$_2$, before and after 51 cycles of electrochemical lithiation. SEM data are shown in Figs. 3*a,b* and in Figs. 3*c,d* before and after lithiation, respectively. The topology of the surface of the electrode after 51/50 cycles of lithiation/delithiation remained practically the same. This can be explained by the stability of this type of crystal structure towards lithiation. The CeNiC$_2$ compound, contrary to metal acetylenides and intermetallic carbides, is stable in air for months. There is also no evidence for significant amounts of Li precipitated on the surface of the grains, as there are no dark regions in Figs. 3*c,d* (light elements give black or dark areas on the SEM-image at the regime of back-scattering electrons). The composition of the grains (averaged over 5 points)

according to EDX analysis showed a small decrease of the carbon content in the sample after lithiation (Ce$_{24.9}$Ni$_{24.2}$C$_{50.9}$ before the electrochemical process, Ce$_{25.2}$Ni$_{24.6}$C$_{50.2}$ after it). A by-product of composition Ce$_{22.7}$Ni$_{21.6}$O$_{55.7}$ appeared after the electrochemical lithiation of the sample. This oxide phase probably formed by interaction between grains of the electrode surface and the electrolyte consisting of ethylene carbonate or dimethyl carbonate, which contain –C=O groups. Another by-product is lithium oxide, Li$_2$O, identified based on its oxygen EDX signal. Lithium oxide was formed by partial oxidation of lithium on the surface of grains.

Our studies revealed two different mechanisms of electrochemical lithiation in the two ternary cerium 3*d*-element carbides studied to date: Ce$_2$Mn$_{17}$C$_{1.77}$ [3] and CeNiC$_2$. As it was shown by Besenhard [1], according to the stoichiometries and crystal structure peculiarities these two compounds belong to two different groups of ternary carbides containing rare-earth and transition elements – metal-rich carbides or intermetallics and carbometalates, respectively. Metal-rich carbides contain single carbon atoms occupying octahedral voids in their structures. This is likely to be the reason for the decarbonization of Ce$_2$Mn$_{17}$C$_{1.77}$ (C content 8.5 at.%) upon electrochemical lithiation-delithiation. Differently, CeNiC$_2$, containing much more carbon (50 at.%), is very stable towards lithiation. The carbon atoms are arranged in C$_2$ groups with strong C=C covalent bonds. These groups are also strongly bonded to Ni atoms forming [Ni(C$_2$)]$_\infty^{n-}$ atomic layers in the structure (see Fig. 4). This is a reason for the stability of the crystal structure toward electrochemical lithiation. However, a small amount of lithium, up to 0.115 Li/f.u., was reversibly incorporated into CeNiC$_2$. The electrochemical lithiation included two reactions: 1) insertion of Li into suitable voids and channels of near-surface layers of CeNiC$_2$, and 2) partial decarbonization of the electrode.

Conclusions

Electrochemical lithiation of CeNiC$_2$ was carried out in a Swagelok-type cell with a positive electrode containing LiCoO$_2$ over 51/50 cycles of lithiation/delithiation. The crystal structure of CeNiC$_2$ (structure type CeNiC$_2$, Pearson symbol *oS*8, space group *Amm*2), before and after lithiation, was investigated by X-ray diffraction (XRD). The electrode containing the ternary carbide was examined by scanning electron microscopy (SEM) and energy-dispersive X-ray spectroscopy (EDX).

The crystal structure of CeNiC$_2$ is very stable toward electrochemical lithiation, contrary to another ternary compound, Ce$_2$Mn$_{17}$C$_{1.77}$, which was studied earlier. A reversible amount of lithium of up to 0.115 Li/f.u. was incorporated into CeNiC$_2$.
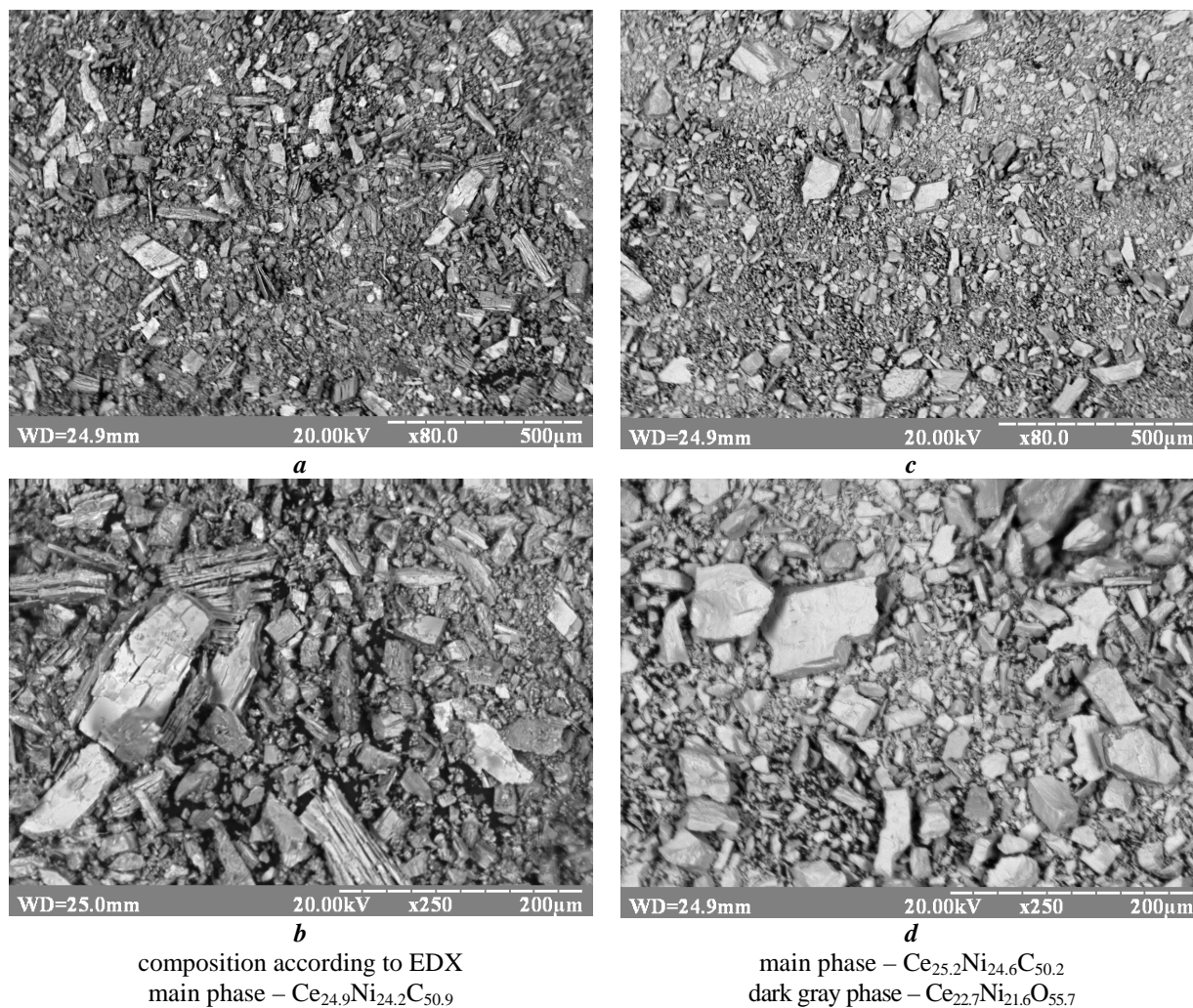
a

c

b

d

composition according to EDX
main phase – Ce$_{24.9}$Ni$_{24.2}$C$_{50.9}$

main phase – Ce$_{25.2}$Ni$_{24.6}$C$_{50.2}$
dark gray phase – Ce$_{22.7}$Ni$_{21.6}$O$_{55.7}$

Fig. 3 Back-scattered electron images of the electrode based on CeNiC$_2$ before (*a*, *b*) and after (*c*, *d*) 51/50 cycles of lithiation/delithiation.
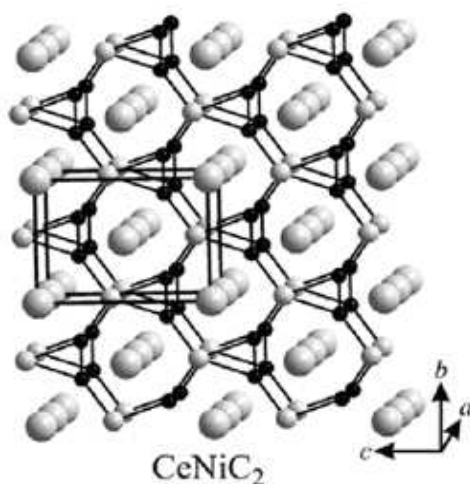

Fig. 4 Crystal structure of CeNiC$_2$. The unit cell is indicated and the atoms forming [Ni(C$_2$)]$_\infty^{n-}$ sheets perpendicular to the *a*-direction are connected by lines. Large gray, small gray and small black balls are Ce, Ni and C atoms, respectively.

The electrochemical lithiation process of CeNiC$_2$ included two reactions: 1) insertion of Li into suitable voids and channels of near-surface layers of CeNiC$_2$, and 2) partial decarbonization of the electrode. The volume of the unit cell of CeNiC$_2$ after 51 lithiation cycles had decreased by 0.06 %. The composition and morphology of the grains of the electrode material had changed slightly. By-products of the lithiation were Li$_z$C$_y$, Ce$_{22.7}$Ni$_{21.6}$O$_{55.7}$ and Li$_2$O. However, their amounts were very small.

The different lithiation mechanisms of CeNiC$_2$ and Ce$_2$Mn$_{17}$C$_{1.77}$ were discussed taking into account peculiarities of their compositions and crystal structures.

Acknowledgments

powder patterns, and to Mr. R. Serkiz (Scientific-Technical and Educational Center of Low-Temperature Studies, Ivan Franko National University of Lviv) for the SEM and EDX analyses.

References

[1] J.O. Besenhard, *Handbook of Battery Materials*, Wiley-VCH, Weinheim, 1999.

[2] C.A. Vincent, B. Scrosati, *Modern Batteries: An Introduction to Electrochemical Power Sources*, 2nd Edition, Arnold, London, 1997.

[3] M. Hembara, V. Kordan, V. Pavlyuk, B. Kotur, *Chem. Met. Alloys* 10 (2017) 45-49.

[4] O.I. Bodak, E.P. Marusin, *Dopov. Akad. Nauk Ukr. SSR, Ser. A* (12) (1979) 1048-1050 (in Ukrainian).

[5] V. Babizhetskyy, B. Kotur, V. Levytskyy, H. Michor, *Chapter 298: Alloy Systems and Compounds Containing Rare Earth Metals and Carbon*, in: J.-C.G. Bünzli, V.K. Pecharsky (Eds.), *Handbook on the Physics and Chemistry of Rare Earths Including Actinides*, North-Holland, Amsterdam, 2017, pp. 1-263.

[6] Stoe & Cie. STOE Win XPOW (Version 2.10), 2004.

[7] L. Akselrud, Y. Grin, *J. Appl. Crystallogr.* 47 (2014) 803-805.

[8] http://chem.lnu.edu.ua/mtech/mtech.htm.

[9] G.B. Bokyy, *Kristallokhimiya*, Moscow, Nauka, 1971 (in Russian).

[10] A. Balińska, V. Kordan, R. Misztal, V. Pavlyuk, *J. Solid State Electrochem.* 19(8) (2015) 2481-2490.

[11] V. Kordan, O. Zelinska, V. Pavlyuk, *Visn. Lviv. Univ., Ser. Khim.* 58(1) (2017) 108-116 (in Ukrainian).

[12] N. Tian, Y. Gao, Y. Li, Zh. Wang, X. Song, L. Chen, *Angew. Chem. Int. Ed.* 55 (2016) 644-648.

[13] N. Tian, Ch. Hua, Zh. Wang, L. Chen, *J. Mater. Chem. A* 3 (2015) 14173-14177.

[14] J. He, X. Song, W. Xu, Y. Zhou, M. Seyring, M. Rettenmayr, *Mater. Lett.* 94 (2013) 176-178.